A combustion mode identification index for multi-regime reacting flows

Lorenzo Angelilli, Francisco E. Hernandez-Perez, Hong G. Im
King Abdullah University of Science and Technology
Thuwal, 23955 Makkah, Saudi Arabia

1 Introducion

The canonical classification of combustion regimes based only on the initial mixture is generally insufficient to describe the combustion processes in complex configurations. In these cases, the effects of the turbulent mixing lead to the coexistence of regimes and local multiple combustion modes.

Recently, Butz *et al.* [1] developed a multi-regime burner (MRB), which is composed of a core jet, two different pilots, and a bluff body. The bluff body, whose wall temperature is kept constant to avoid re-condensation close to the nozzle exits, allows the inhomogeneous conditions to develop thanks to the onset of a recirculation region and the consequently enhanced turbulence generated by mixing layer interaction. This configuration is suitable for the experimental investigation of multi-regime combustion under well-controlled conditions [1] as well as for validating combustion models.

In a first attempt to model a multi-regime flame of the MRB configuration, Popp *et al.* [2] conducted a large eddy simulation (LES) and employed the artificially thickened flame (ATF) model [3] to model the chemical source term. Nevertheless, the prediction of the CO mass fraction and temperature at the far field displayed noticeable deviations, indicating deficiencies in the modeling approach. Due to the importance of the chemistry source term to correctly predict the local extinction/re-ignition and the various flame regimes, a finite-rate-based chemistry model would appear to be more suitable, particularly in the limit of fully resolved simulations.

The goal of this manuscript is to assess the combustion regimes that occur in the MRB configuration employing LES. To track the the thermochemical properties in time, massless Lagrangian particles that evolve with the filtered velocity are randomly injected from the nozzle exits. Subsequently, on the basis of the multi-modal manifold developed by Mueller *et al.* [4, 5], a novel combustion mode index is proposed and applied to the Lagrangian particles in order to uniquely characterize the regime along a particle trajectory. In contrast with other methods such as the flame index of Yamashita *et al.* [6], which assumes that the regime information is embedded only in the alignment between fuel and oxidizer gradients, or the gradient free regime identification (GFRI) algorithm [7], which only provides a qualitative description of the flame regions, the proposed index offers a quantitative description of the combustion regime.

Correspondence to: lorenzo.angelilli@kaust.edu.sa

2 Numerical model

This section describes the mathematical framework employed in this work. In particular, the LES framework sub-models used to perform the simulations campaign, the multimodal manifold equations, and the regime classification criteria are explained in detail.

Large eddy simulations (LES) only resolve the larger scales of the gas phase behavior, and the contribution of the unresolved part is captured by the sub-grid scales (SGS) models [8]. The turbulent closures of the Leonard stress tensor have been extensively investigated in the last decades. The wall-adaptive eddy viscosity (WALE) [9] model was an excellent candidate to capture the effect of the bluff body on the sub-grid scales.

Additionally, we assume that the Lewis number (Le$= \lambda/(\rho C_p D)$) is constant and approximated to the unity. This hypothesis is justified by the fact that the main fuel is methane. The chemical source term is directly computed by the Arrhenius law, and the sub-grid scales are closed by employing the eddy dissipation concept.

Lagrangian particles are randomly injected at the different inflow exits and evolve according to the equation

$$\frac{D\mathbf{X}_p}{Dt} = \widetilde{\mathbf{U}} \tag{1}$$

following the resolved scales of the fluid motion. The particles track the evolution of temperature, pressure, species mass fractions, diffusion, and chemical source terms.

We identify the combustion regimes by comparing the reacting evolution of a single particle in the mixture fraction and progress variable space the physically derived manifold (PDR) for multimodal combustion [4]. In the PDR context, the chemical state space is a two-dimensional function of the mixture fraction, Z, and the generalized progress variable, Λ. Mixture fraction and progress variable take on values between zero and the unity, where $Z = 0$ corresponds to the oxidizer stream, $Z = 1$ corresponds to the fuel stream, $\Lambda = 0$ corresponds to the unburnt mixture, and $\Lambda = 1$ equals the mixture at the thermochemical equilibrium. Such description allows representing both the premixed and non-premixed regimes simultaneously as an asymptotic behavior of the mathematical derivation.

Given a reference species, the generalized progress variable is defined as

$$\Lambda = \frac{C - C_u(Z)}{C_{eq}(Z) - C_u(Z)}, \tag{2}$$

where $C_u(Z)$, $C_{eq}(Z)$ and C are progress variable of the unburned mixture at a given Z, at equilibrium at a given Z, and at the local condition, respectively. Following the canonical definition of progress variable for methane formulated by Pierce et al. [10], we have

$$C = Y_{H2O} + Y_{CO2} + Y_{CO} + Y_{H2}. \tag{3}$$

Employing the nonlinear reference [5] for the generalized progress variable, the asymptotic combustion modes are fully recovered. The reader can find the entire PDR formulation in Refs. [4, 5].

The multi-regime burner (denoted as MRB) geometry is described in Ref. [1], and consists of three coaxial jets (denoted as *jet*, *slot 1*, and *slot 2*) that can operate independently with different equivalent ratios. Slot 1 injects pure air at 15 m/s, slot 2 a lean mixture of air and methane at the equivalence ration of $\phi = 0.8$ at 20 m/s, and the coflow is composed of pure air at 1 m/s. We performed a campaign of two simulations corresponding to the experimental cases 18b and 26b [1] where the composition of the central jet is a mixture of air and methane at $\phi = 1.8$ and 2.6, respectively, whereas the bulk velocity is 105 m/s. The validation of the simulation campaign, together with a sensitivity study of the solution to the chemical kinetic model, was assessed by Angelilli *et al.* [11].

3 Mode identification index formulation

The multimodal combustion approach [4, 5] is adequate to describe the peculiar flame structure because it includes the effects of varying mixture fraction and residence time in its formulation. To represent the particle trajectories in the state space composed of the mixture fraction Z and the generalized progress variable Λ, we define a curvilinear coordinate as

$$\xi(t) = \oint_{t_0}^{t} ||\mathbf{S_p}'(Z(\tau), \Lambda(\tau))|| d\tau \tag{4}$$

where $\mathbf{S_p}(Z(\tau), \Lambda(\tau))$ is the position vector in the state space (Z, Λ), and the superscript $'$ indicates the derivate of $\mathbf{S_p}$ respect to the time. Physically, the curvilinear coordinate ξ is a representation of a pseudotime of the particle evolution in the state space.

Recalling the nonlinear reference for the state space (Z, Λ) explained in detail by Novoselov *et al.* [5], we can correlate the trajectory in the state space to the combustion regime. On one hand, if $d\Lambda/d\xi = 0$ and $dZ/d\xi \neq 0$, the flame is purely nonpremixed or is a pure mixing if $\Lambda = 0$. On the other hand, if $d\Lambda/d\xi \neq 0$ and $dZ/d\xi = 0$, we have a purely premixed flame at the equivalence ratio function of the mixture fraction. Then, we can differentiate the combustion regimes according to the slope of the particle trajectory and a novel mode identification index is proposed:

$$\theta_R = \arctan\left(\frac{d\Lambda/d\xi}{\text{sign}(Z - Z_{st}) dZ/d\xi}\right). \tag{5}$$

In addition, it is remarkable that if $\text{sign}(Z_{st} - Z) dZ/d\xi > 0$, the particle is approaching the stoichiometric; otherwise, it is diluting, independently from being on the rich or lean side of the flame.

Figure 1 summarizes the polar representation of the possible combustion regimes with θ_R varying between $-\pi$ and π. Then, both $\theta_R/\pi = -1$ and $\theta_R/\pi = 1$ indicates the nonpremixed diluting limit, $\theta_R/\pi = 0.5$ the premixed limit, $\theta_R/\pi = 0$ the nonpremixed limit where $Z \to Z_{st}$, and $\theta_R/\pi = -0.5$ the pure premixed quenching. Furthermore, we can assess that if $\theta_R/\pi > 0$ the particle burns; otherwise, the flame tends to extinction, and if $-0.5 < \theta_R/\pi < 0.5$ the mixture becomes more reactive because it tends to the stoichiometric limit; otherwise it is more diluted. The circular sectors of the diagrams represent the intermediate conditions given by a combination of multiple regimes.

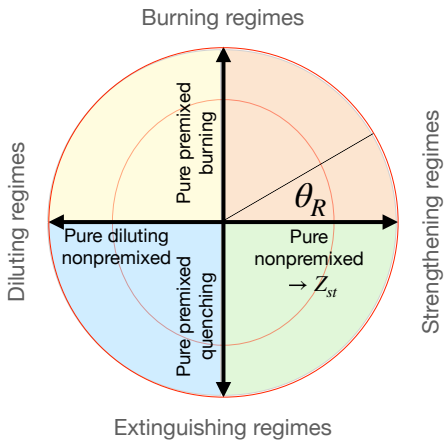

Figure 1: Summary of the polar representation of the combustion regimes.

To describe back-lean and back-rich supported regimes, an additional flammability index (FI) is defined as follows:

$$FI = \text{sign}(Z - Z_{st})\mathcal{H}(Z_{st} - Z)\left(\frac{Z - Z_{st}}{Z_{fl}^{L} - Z_{st}}\right) + \text{sign}(Z_{st} - Z)\mathcal{H}(Z - Z_{st})\left(\frac{Z - Z_{st}}{Z_{fl}^{R} - Z_{st}}\right) \tag{6}$$

where Z_{fl}^{R} and Z_{fl}^{L} are the rich and lean flamability limits, and $\mathcal{H}(\cdot)$ is the Heaviside function. Then, $FI < 0$ indicates a lean mixture, otherwise a rich one. If $\theta_R/\pi > 0$, for $FI < -1$ we have the back-lean supported regime, and $FI > 1$ represents the back-rich supported regime.

4 Preliminary results

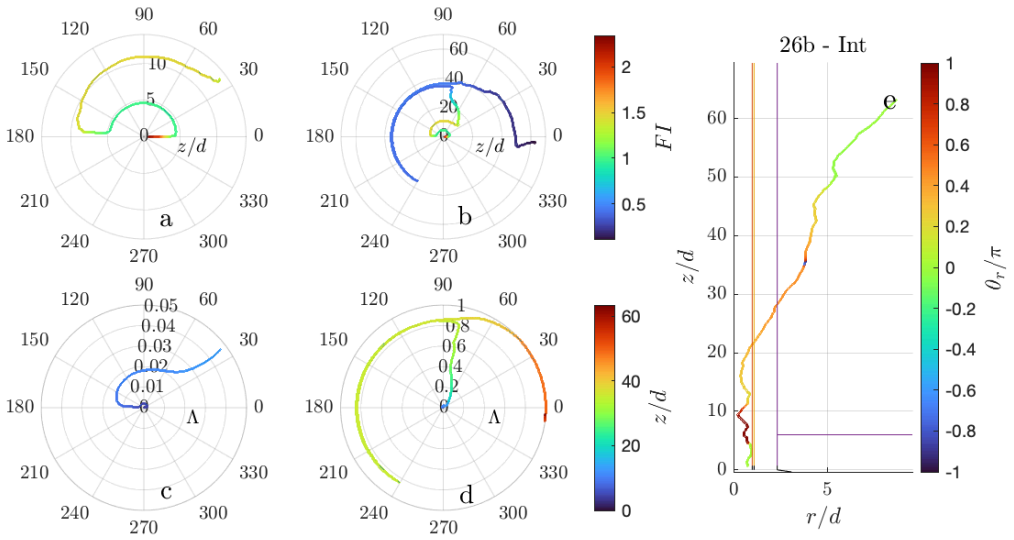

Figure 2: Evolution of Lagrangian particle of 26b case exiting from central jet. Panels a and b: polar description of $\theta_R(z/d)$, panels c and d : polar description of $\theta_R(\Lambda)$, panel e: particle trajectory in physical space.

Figure 2 is detailed representation of a Lagrangian particle exiting from the internal jet of the case 26b. In particular, the panel on the right describes the scatter plot of the particle trajectory colored with the value of θ_R/π. For $z/d < 10$ the particle is experiencing pure mixing between, for $10 < z/d < 40$ we observe a premixed ignition and for $z/d > 40$ the particle experience a nonpremixed combustion. The combustion dynamics is detailed in the polar diagrams (panels a-d). Figure 2a and fig. 2c focuses on the region $z/d < 13$, whereas fig. 2b and fig. 2d on the entire domain. At the injection (fig. 2a and c) the particle rich ($FI \approx 2$) and for $z/d < 2.5$ the strong diffusion with the pure air exiting from the slot 1 contributes to reduce $FI \approx 1$, then a premixed ignition occurs at $z/d \approx 5$ ending a nonpremixed enriching combustion for $5 < z/d < 10$ where the flammability index increases to $FI \approx 1.5$. During this processes Λ slightly increases to 0.01 suggesting that these are the initial steps of the ignition. At $z/d \approx 10$ the combustion regime switches from nonpremixed to multimodal (θ_R/π decreases from 1 to ≈ 0.25), Λ increases to 0.02 and $FI \approx 1.5$. Since $\theta_R/\pi > 0$ and $FI \approx 1.5$, for $10 < z/d < 11$ the regime is back-rich supported. Successively, from $11 < z/d < 25$ we observe multimodal ignition where Λ increases to 0.2 and then a dominantly premixed burning for $25 < z/d < 40$ with Λ up to 0.8, the flammability index becomes less than 0.5 making the mixture more reactive. At $z/d \approx 40$ a local extinctio and re-ignition driven by diffusion occurs (θ_R/π rapidly varying from 0.4 to -0.66 crossing the line of nonpremixed diluted regime). We assist to a multimodal re-ignition ($\theta_R/\pi \approx 0.25$)

at $40 < z/d < 50$ where the mixture achives the chemical equilibrium $\Lambda \approx 1$ and then we have a nonpremixed combustion tending to the stoichiometric around the equilibrium for $z/d > 50$.

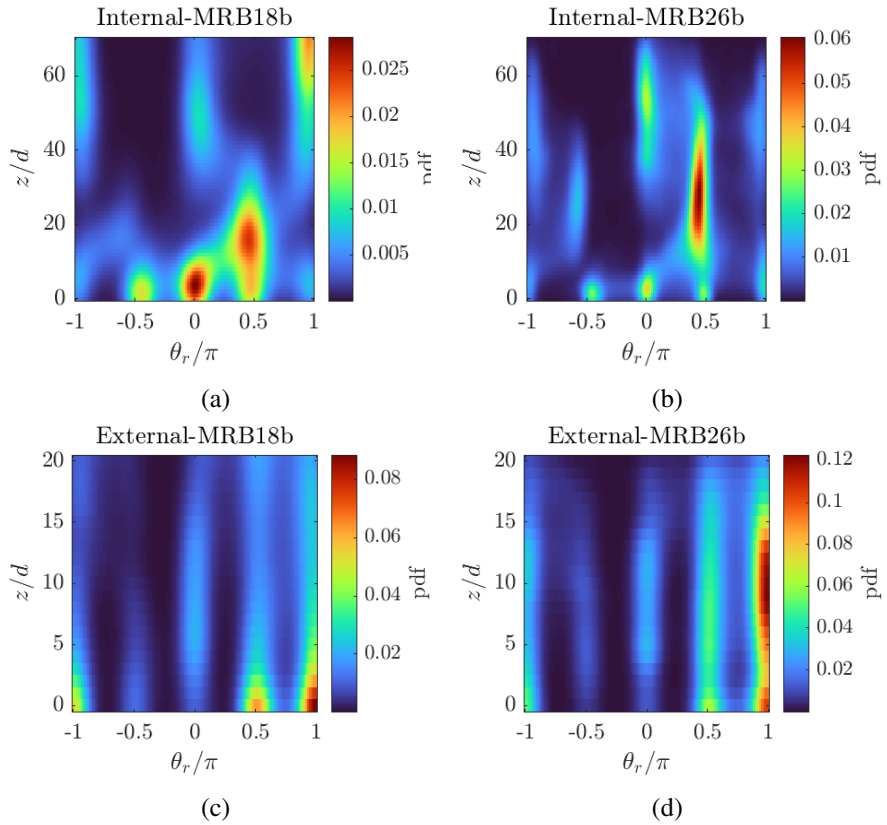

Figure 3: Joint probability density function of $(\theta_R/\pi, z/d)$ for central jet particles (panels a and b) and external particles (panels c and d), case 18b (panels a and c) and case 26b (panels b and d).

Figure 3 reports the joint-pdf between z/d and θ_R/π obtained from a collection of 200 injected Lagrangian particles. Panels a and b display the characteristics of the internal flame, and c and d for the external one for the configurations 18b and 26b, respectively. On the one hand, the internal flame of the 18b case shows that at the initial stages of the flame $z/d < 20$, the particles experience an intenser mixing than in the 26b case and the premixed ignition region is shorter with a stronger multimodal transition. Furthermore, in the 26b case, premixed and nonpremixed regimes coexist for $30 < z/d < 50$, whereas case 18b shows a smooth transition at $z/d \approx 30$. Furthermore, for $z/d > 40$, case 26b shows in prevalence the nonpremixed regime tending to stoichiometric conditions, whereas in case 18b, the diluting conditions. Remarkably, the dilution is the final step of nonpremixed combustion of a fluid particle before entering the fresh air region. This suggests that the reacting zone in the 26b case is larger than 18b. The back-supported regimes that can be identified by $\theta_R/\pi \approx 0.5$ at $z/d < 5$ are more probable in the leaner case 18b because of the coexistence of intenser mixing $\theta_R/\pi \approx 0$.

Figures 3c and d display that the external flames are purely premixed with a low probability of nonpremixed and quenching ($\theta_R/\pi \approx 0$ and ≈ -0.5) consistently between the two cases. It is worth recalling that the likelihood of finding $\theta_R/\pi \approx 1$ at the initial stages refers to the particles injected from slot 2 that are advected outside the core jet region and remain composed of fresh gases. This probability is consistent between the two cases because the inflow conditions in slot 2 are similar. Case 18b shows that most particles burn in the premixed regime only within the recirculating zone. In contrast, case 26b shows a higher probability of premixed combustion and nonpremixed dilution for $z/d > 5$, signifying

that the different jet composition can affect the topology of the external flame far field. These results are similar to the experimental findings in [2].

5 Conclusion

This extended abstract presented a novel regime classification indexes based on the slope of Lagrangian tracking particles in the state space formed by the mixture fraction and the generalized progress variable. The index, together with the polar representation of the trajectory, is able to identify all combustion modes and extinction re-ignitions. The joint pdf showed that the identified regime are similar to the experimental findings.

References

[1] David Butz, Sandra Hartl, Sebastian Popp, Steffen Walther, Robert S. Barlow, Christian Hasse, Andreas Dreizler, and Dirk Geyer. Local flame structure analysis in turbulent ch4/air flames with multi-regime characteristics. *Combustion and Flame*, 210:426 – 438, 2019.

[2] Sebastian Popp, Sandra Hartl, David Butz, Dirk Geyer, Andreas Dreizler, Luc Vervisch, and Christian Hasse. Assessing multi-regime combustion in a novel burner configuration with large eddy simulations using tabulated chemistry. *Proceedings of the Combustion Institute*, 38(2):2551–2558, 2021.

[3] O Colin, Frédéric Ducros, D Veynante, and Thierry Poinsot. A thickened flame model for large eddy simulations of turbulent premixed combustion. *Physics of fluids*, 12(7):1843–1863, 2000.

[4] Michael E Mueller. Physically-derived reduced-order manifold-based modeling for multi-modal turbulent combustion. *Combustion and Flame*, 214:287–305, 2020.

[5] Alex G Novoselov, Bruce A Perry, and Michael E Mueller. Two-dimensional manifold equations for multi-modal turbulent combustion: Nonpremixed combustion limit and scalar dissipation rates. *Combustion and Flame*, 231:111475, 2021.

[6] H Yamashita, M Shimada, and T Takeno. A numerical study on flame stability at the transition point of jet diffusion flames. In *Symposium (international) on combustion*, volume 26, pages 27–34. Elsevier, 1996.

[7] David Butz, Sandra Hartl, Sebastian Popp, Steffen Walther, Robert S Barlow, Christian Hasse, Andreas Dreizler, and Dirk Geyer. Local flame structure analysis in turbulent ch4/air flames with multi-regime characteristics. *Combustion and Flame*, 210:426–438, 2019.

[8] Stephen B Pope. Turbulent flows, 2001.

[9] FR Menter and Y Egorov. The scale-adaptive simulation method for unsteady turbulent flow predictions. part 1: theory and model description. *Flow, Turbulence and Combustion*, 85(1):113–138, 2010.

[10] C.D. Pierce and P. Moin. Progress-variable approach for large-eddy simulation of non-premixed turbulent combustion. *Journal of Fluid Mechanics*, (504):73–97, 2004. cited By 761.

[11] Lorenzo Angelilli, Pietro Paolo Ciottoli, Francisco E Hernandez Perez, Mauro Valorani, Hong G Im, and Riccardo Malpica Galassi. Large eddy simulation of multi-regime burner: a reaction mechanism sensitivity analysis. In *AIAA SCITECH 2022 Forum*, page 0639, 2022.